Magnetic properties of $Fe_2O_3(0001)$ thin layers studied by soft x-ray linear dichroism

Susana Gota* and Martine Gautier-Soyer
CEA/Saclay, DSM/DRECAM/SPCSI, Service de Physique et de Chimie des Surfaces et des Interfaces, 91191 Gif-sur-Yvette Cedex, France

Maurizio Sacchi
Laboratoire pour l'Utilisation du Rayonnement Electromagnétique, Centre Universitaire Paris-Sud, Boîte Postale 34, 91898 Orsay, France

(Received 30 March 2001; published 20 November 2001)

X-ray magnetic linear dichroism (XMLD) at the Fe L_2 absorption edge has been used for investigating the magnetic properties of thin epitaxial α-Fe_2O_3 layers (20 and 80 Å thick). When cooling below 263 K, bulk hematite undergoes a 90° rotation of the antiferromagnetic axes from perpendicular to parallel to the *c* axis (Morin transition). The L_2-XMLD results indicate that the 80-Å-thick layer does not undergo such a transition at least down to 125 K. This absence is attributed to important magnetoelastic interactions due to the 0.3% expansion of the lattice parameter in the *c* plane. In the case of a 20-Å-thick layer, we do not detect any L_2-XMLD signal, regardless of the temperature. The absence of antiferromagnetic ordering might be caused by the combined effect of several factors: finite size effects, changes in the local crystal field of the Fe^{3+} ion, and magnetoelastic interactions, coming from the 0.8% expansion of the lattice parameter in the *c*-plane.

DOI: 10.1103/PhysRevB.64.224407 PACS number(s): 75.50.Ee, 75.70.Ak, 78.70.Dm

I. INTRODUCTION

Antiferromagnetic (AF) layers of nanometric dimensions play an important role in the development of magnetoelectronic devices. For instance, they are used for pinning soft ferromagnetic (*F*) layers by exchange biasing in spin-valve devices.[1,2] Despite their importance in the information-storage technologies, the microscopic mechanism of the magnetic coupling between AF-*F* adjacent layers is not well understood.[3,4] A preliminary step for making progress in this direction is to probe each magnetic layer in detail.

Nanometric AF layers pose some peculiar technical problems. Their zero net magnetic moment, along with the extremely reduced amount of material, make many traditional tools in magnetometry ineffective to their investigation. X-ray magnetic linear dichroism (XMLD), which consists in the difference in absorption cross section for light linearly polarized perpendicular or parallel to the local magnetic moment **M**, is proportional to $\langle \mathbf{M}^2 \rangle$, so it is sensitive to any collinear magnetic ordering, whether it be *F* or AF. In addition, being based on a core-level resonant process, XMLD is an element-specific probe of magnetization. Very recently, photo-electron emission microscopy (PEEM) combined with XMLD spectroscopy has been successfully used to image the AF domains of NiO(100) (Ref. 5) and $LaFeO_3$ (Ref. 6) thin films. Also, using both XMLD and XMCD (x-ray magnetic circular dichroism) contrast, PEEM experiments have revealed the magnetic coupling in a Co/$LaFeO_3$ bilayer.[7]

AF oxides exhibit higher ordering temperature and better thermal stability than AF metals, and their use for exchange bias applications has proven successful. Controlled growth methods for engineering oxide layers at the atomic scale are currently under intense development.[8]

Within this framework, we focused our interest on the magnetic properties of hematite (α-Fe_2O_3) thin films, an AF oxide that has already been used in magnetic tunnel junctions.[9] Even if the magnetic properties of bulk α-Fe_2O_3 samples have been extensively studied in the past,[10,11] the magnetic behavior of ultrathin layers can be rather different from that established for the bulk form. It has been recently shown that the Néel temperature (T_N) of other AF oxides as NiO,[12,13] CoO,[13] and $LaFeO_3$ (Ref. 6) strongly depends on the layer thickness and on the lattice parameter strain caused by epitaxial growth.

α-Fe_2O_3 crystallizes in the rhombohedral crystal structure. This structure can be indexed either as rhombohedral ($\alpha = 55°17'$ and $a = 5.420$ Å) or hexagonal ($a_0 = 5.034$ Å and $c_0 = 13.749$ Å). In the bulk form, hematite exhibits a high Néel temperature ($T_N^{\mathrm{Bulk}} = 953$ K) and then it is AF ordered at room temperature (RT). The iron moments are *F* ordered in the hexagonal basal planes, the moments pointing towards the nearest iron neighbors. The *F*-ordered (0001) planes form a +, −, −, + sequence along the trigonal axis, resulting in a net AF order.[14] In absence of an external magnetic field, α-Fe_2O_3 exhibits three AF domains, obtained by a $\pm 120°$ rotation of a single domain around the trigonal axis.[15,16] An anisotropic spin-spin interaction cants the two sublattices of opposite magnetization towards each other and hence leads to a weak spontaneous magnetization in the basal plane.[17,18]

As a function of temperature, hematite undergoes a magnetic reorientation transition resulting in a 90° rotation of the AF axis from parallel to perpendicular to the basal plane, called Morin transition (MT).[19] In bulk samples, it occurs when cooling down to $T_M^{\mathrm{Bulk}} \approx 263$ K. Below T_M, the moments are perfectly aligned along the threefold *c* axis and the weak ferromagnetic component disappears.

The reorientational MT has been used by Kuiper *et al.* to demonstrate the pure magnetic origin of the large XMLD signal measured at the Fe $L_{2,3}$ edges in a α-Fe_2O_3 single crystal.[20] Taking their work as a starting point, we use XMLD for studying the magnetic properties of α-$Fe_2O_3(0001)$ in the thin layer form.

II. EXPERIMENTAL METHODS

Our analysis relies on the comparison between the XMLD results for a α-$Fe_2O_3(0001)$ single crystal and two layers 20 and 80 Å thick. All samples exhibit high crystalline order and surfaces oriented parallel to the basal plane.

The single crystal was a high quality (0001)-oriented platelet, grown by the flux method at the Clarendon Laboratory (Oxford). Its size was about $5\times5\times1$ mm^3. The 20- and 80-Å-thick layers were grown epitaxially on an α-$Al_2O_3(0001)$ single crystal by atomic-oxygen-assisted molecular beam epitaxy (O-MBE). α-Al_2O_3 exhibits the same rhombohedral corundum crystal structure than α-Fe_2O_3. O-MBE permits to control the structure and stoichiometry of the oxide layer at the atomic scale. Our experimental ultrahigh vacuum setup is equipped with an iron Knudsen cell and an oxygen plasma source (OPS), both having their effusion beam axes converging on the sample. The OPS and the deposition procedure are extensively described in previous references.[21–23] During the growth, the substrate was kept at RT. The film thickness was calibrated by means of the oscillations of the RHEED (reflexion high-energy electron diffraction) specularly reflected intensity. The thin layers and the single crystal were postannealed at 1000 K under controlled O_2 atmosphere ($PO_2=10^{-6}$ mbar). After this treatment, they exhibit high-quality LEED (low energy electron diffraction) and RHEED patterns corresponding to α-$Fe_2O_3(0001)$.[21,22] *In situ* X-ray photoemission spectroscopy analysis confirms that solely Fe^{3+} ions are present in the samples. From *in situ* RHEED (Refs. 22 and 23) and *ex situ* grazing incidence x-ray diffraction (GIXRD), [21,22] we found an expansion of the lattice parameter in the *c* plane of $\Delta a_0/a_0=0.3\%$ and 0.8%, respectively, for the 80- and 20-Å-thick layers. RHEED and GIXRD cannot give direct information about interatomic distances along the *c* axis.

The Fe $L_{2,3}$ spectra were recorded on the SA22 beamline of the storage ring SuperACO at LURE (Orsay, France). Before the XMLD experiment, the samples were annealed at 1000 K in 10^{-6} Torr of O_2 for restoring surface stoichiometry and crystallinity. After annealing, all the samples exhibited LEED patterns characteristic of a α-$Fe_2O_3(0001)$ surface over a wide energy range (80–250 eV).

SA22 is a bending magnet beamline equipped with a plane grating monochromator, covering the 400–800 eV energy range with a maximum resolving power of $E/\Delta E=3500$. The Fe $L_{2,3}$ x-ray absorption spectra were measured in the total electron yield (TEY) mode using a channeltron placed in front of the irradiated sample. Linearly polarized light was obtained by selecting a narrow vertical accepted angle symmetrical with respect to the orbit plane of the positrons in the ring. The sample was placed vertically in front of the photon beam, and the manipulator permitted its rotation around the vertical axis. The sample was cooled by liquid N_2 circulating in a copper reservoir in contact with the back of the sample holder. A thermocouple welded on the sample holder measured the temperature. The lowest-reached temperature that will be indicated as LN in the following, was actually of about 125 K at the sample position.

Figure 1 illustrates the experimental geometries used in this work. $\boldsymbol{\varepsilon}$ denotes the electric-field vector of the photon beam of energy $h\nu$, $\hat{c}$ the surface normal (which coincides with the trigonal axis), and θ the angle between $\boldsymbol{\varepsilon}$ and $\hat{c}$. Thick arrows (**A**) indicate the AF axes. We have recorded the Fe $L_{2,3}$ spectra at two photon beam incidences:

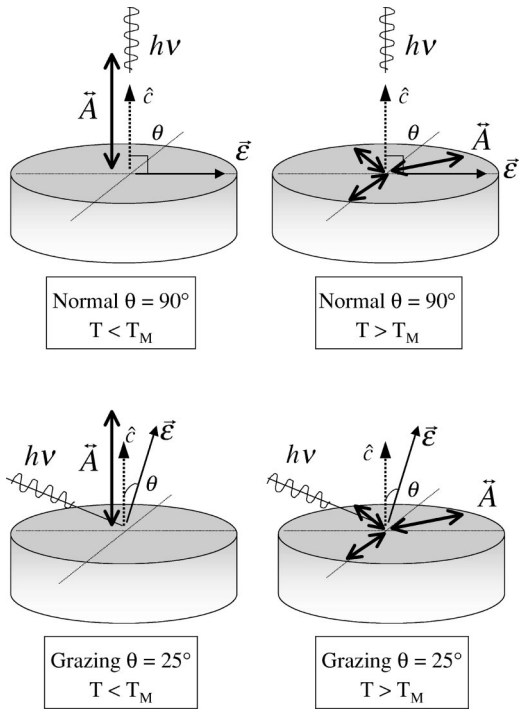

FIG. 1. Schematic representation of the experimental geometries used in this work. $\boldsymbol{\varepsilon}$ denotes the electric-field vector of the photon beam of energy $h\upsilon$, $\hat{c}$ the surface normal (which coincides with the trigonal axis), and θ the angle between $\boldsymbol{\varepsilon}$ and $\hat{c}$. Thick arrows (**A**) indicate the antiferromagnetic axes. Top panels correspond to normal incidence ($\theta=90°$) and bottom panels to grazing incidence ($\theta=25°$). For both incidences, the antiferromagnetic axes are schematized for $T<T_M$ (left panels) and for $T>T_M$, (right panels) in the hypothesis of the ideal magnetic behavior of a bulk hematite sample.

(a) Normal incidence (NI). The photon beam is perpendicular to the surface. $\boldsymbol{\varepsilon}$ lies in the basal plane and hence $\theta=90°$ (top panels of Fig. 1). At $T<T_M$, $\boldsymbol{\varepsilon}\perp\overline{A}$. At $T>T_M$, the trigonal domains rotated by $\pm120°$ lying down on the basal plane are schematised by three $\overline{A}$ vectors.

(b) Grazing incidence (GI). Ideally $\boldsymbol{\varepsilon}\|\hat{c}$, giving the best sensitivity to the spin reorientation transition in the case of (0001) surface orientations: When $\theta=0°$, the relative orientation between $\boldsymbol{\varepsilon}$ and $\overline{A}$ passes from parallel at $T<T_M$ to perpendicular at $T>T_M$, independently of the existence of trigonal domains. The lower GI angle we could safely use in our experiments was $\theta=25°$ (bottom panels of Fig. 1).

Figure 2 shows the TEY Fe $L_{2,3}$ spectra of the α-$Fe_2O_3(0001)$ single crystal at GI for temperatures above and below $T_M^{\mathrm{Bulk}}=263$ K (RT and LN, respectively). For obtaining the dichroic signal, the row spectra have been analyzed as follows. In a first step, a linear baseline has been subtracted from both spectra. After that, they have been scaled to the background intensity at an energy intermediary

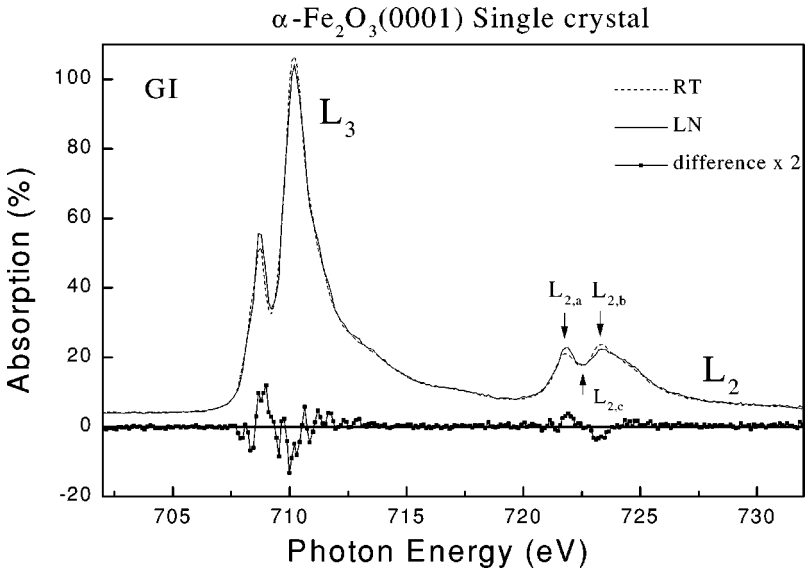

FIG. 2. Fe $L_{2,3}$ spectra of the α-$Fe_2O_3(0001)$ single crystal recorded at GI for temperatures above and below $T_M^{\mathrm{Bulk}}=263\,\mathrm{K}$ (RT and LN, respectively). The difference curve (RT-LN), multiplied by a factor 2, is reported. $L_{2,a}$ and $L_{2,b}$ denote the maximum at the two peaks composing the L_2 edge and $L_{2,c}$ is the midpoint between them. These quantities are used for calculating L_{ratio} (see text).

between the L_2 and L_3 edges. The difference curve (RT-LN) coincides in sign with that of Kuiper *et al.*[20]

The saturation effects intrinsic to the TEY detection mode can be a problem when small XMLD signals are concerned, especially at the GI geometry. In a previous work, we have quantified the angular-dependent saturation effects separately at the Fe L_3 and L_2 edges in the particular case of iron oxides.[24] The conclusion is that the L_3 edge is significantly more disturbed by saturation effects than the L_2 edge. For this reason, in the present work we use exclusively the Fe L_2 edge for measuring XMLD effects.

In order to prove the sensitivity of our experiment to the reorientational Morin transition, we have quantified the Fe L_2-XMLD signal in the case of the α-$Fe_2O_3(0001)$ single crystal. We define L_{ratio} in the following way:

$$L_{\mathrm{ratio}}=\frac{I(L_{2,a})-I(L_{2,c})}{I(L_{2,b})-I(L_{2,c})}, \tag{1}$$

where $I(L_{2,a})$ and $I(L_{2,b})$ are the maximum intensities at the two peaks composing the L_2 edge, and $I(L_{2,c})$ is the intensity in the midpoint between them. These values are determined on the raw spectra, before the data reduction mentioned above.

Figure 3 presents the evolution of L_{ratio} measured on the α-$Fe_2O_3(0001)$ single crystal as a function of temperature going from LN to RT. We can appreciate a variation in the value of L_{ratio} that we correlate with the Morin transition. Although it is not as sharp as expected for a first-order transition, it is known that the Morin transition in single crystals can be rather broad since it takes place through a sequence of abrupt transitions of different regions of the crystal exhibiting slightly different values of T_M.[25] These regions are defined by the amount of impurities incorporated during the growth process. Our measurement gives a mid jump at about $T_M\sim 255\,\mathrm{K}$, which is in good agreement with the values reported for single crystals.

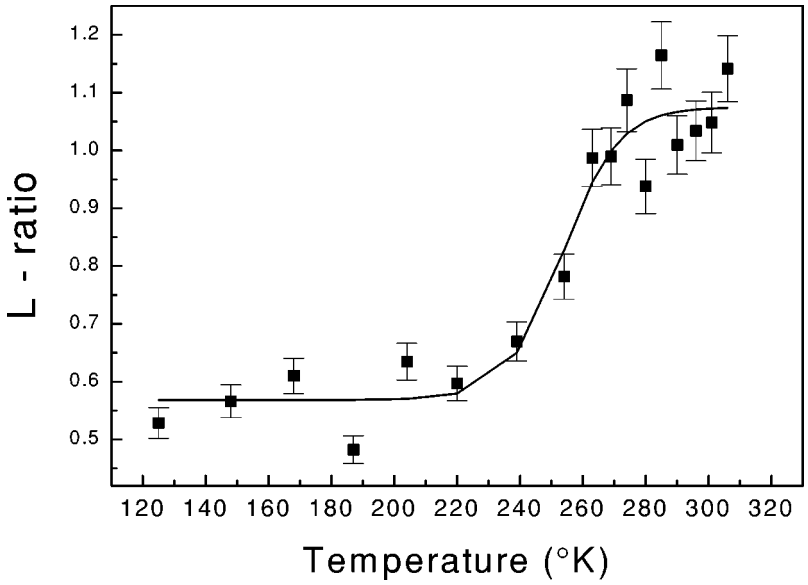

FIG. 3. Evolution of L_{ratio} measured on the α-$Fe_2O_3(0001)$ single crystal as a function of temperature. Spectra were measured at GI.

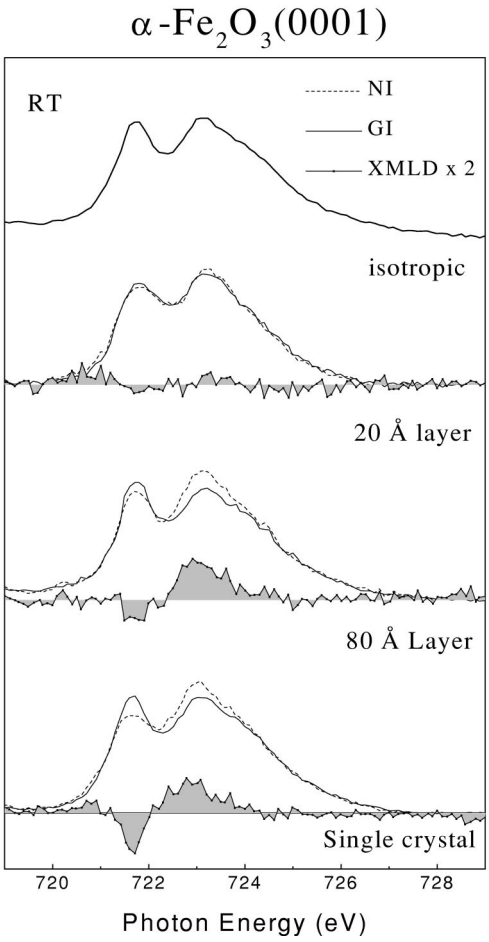

FIG. 4. Fe L_2 spectra recorded at RT corresponding to a α-Fe_2O_3(0001) single crystal and to thin layers of 80 and 20 Å, respectively. The XMLD signals correspond to the differences between the NI and GI geometries and are multiplied by a factor 2. The isotropic spectrum is also included.

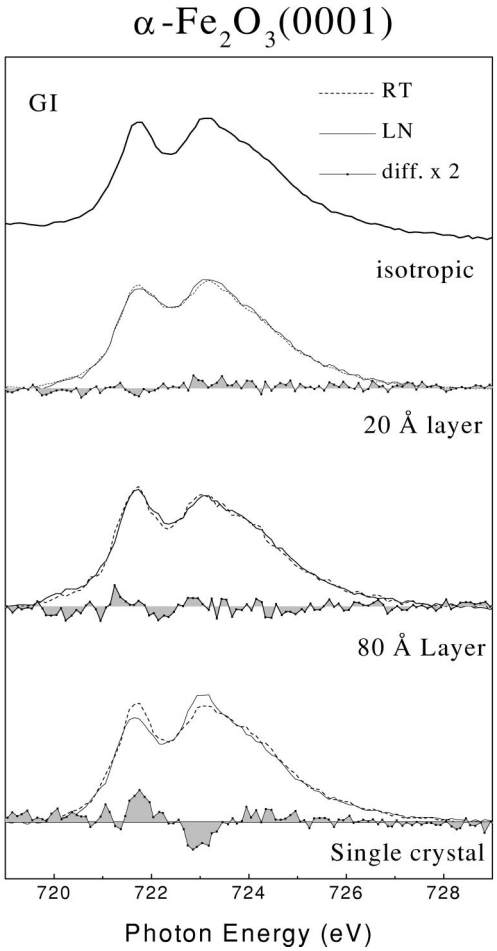

FIG. 5. Fe L_2 spectra, recorded at grazing incidence, corresponding to an α-Fe_2O_3(0001) single crystal and to thin layers of 80 and 20 Å, respectively. The difference signals are taken between the spectra recorded at RT and LN and are multiplied by a factor 2. The isotropic spectrum is also included.

In Fig. 4 we compare the RT Fe L_2 spectra of the α-Fe_2O_3(0001) single crystal, the 80- and the 20-Å-thick layers. The XMLD signals correspond to the differences between the NI and the GI geometries. The isotropic absorption spectrum is also included. We observe that the XMLD signals corresponding to the single crystal and the 80-Å-thick layer are qualitatively the same. On the basis of the results of Kuiper *et al.*,[20] this implies that the 80-Å-thick layer exhibits at RT the AF ordering characteristic of the high-temperature phase of bulk hematite. In contrast, under the same experimental conditions, no XMLD signal is detectable for the 20-Å-thick layer above the noise level. In addition, this latter L_2 line shape is very close to that of the isotropic spectrum. These facts strongly suggest that the 20-Å-thick layer is not magnetically ordered at RT.

In Fig. 5 we compare the GI Fe L_2 spectra corresponding to the α-Fe_2O_3(0001) single crystal, the 80- and 20-Å-thick layers. Shaded curves are the difference between the spectra recorded at RT and at LN. The isotropic spectrum is also included. The sign of the difference for the single crystal indicates that its magnetic moments are well aligned along the threefold axis at LN.[20] The same experiment on the 80-Å-thick layer, yields zero difference within the noise level. This result strongly indicates that the spin reorientation does not occur in the 80-Å-thick layer at least down to 125 K. From the line shape of this L_2 spectrum, we can also infer that the magnetic moments remain parallel to the *c* plane. In the case of the 20-Å-thick layer, no difference signal is detectable between LN and RT. Moreover, the line shape at LN resembles more that of the isotropic spectrum rather than that of the 80-Å-thick layer. This observation confirms that the 20-Å-thick film is not magnetically ordered, even at temperatures as low as 125 K.

III. DISCUSSION

The reorientational Morin transition in hematite is generally explained in the literature using the Artman, Murphy, and Foner (AMF) model.[26] In this formalism, the anisotropy constant K can be expressed as the sum of two opposing contributions $K=K_{MD}+K_{SI}$ coming from different microscopic origins. K_{MD} is the dipolar anisotropy constant and represents the long-range interaction of the Fe^{3+} magnetic

ions. K_{SI} is the single-ion anisotropy constant and describes the effect of the crystal field in the Fe^{3+} magnetic moment. The latter is a short-range interaction due to the spin-orbit coupling. In the AMF model, K_{MD} and K_{SI} have opposite signs and exhibit different temperature dependence. K_{MD} is negative and directs the magnetic axis within the *c* plane, whereas K_{SI} is positive and directs the magnetic axis along the *c* axis.

The reorientational MT is caused by a reversal of the sign of the overall *K* as a function of the temperature. At $T=0$ K, the magnetic moments are aligned parallel to the *c* axis because $K_{SI}>|K_{MD}|$. Nevertheless, at $T=0$ K, K_{SI} is only 2% bigger in magnitude than K_{MD}. As K_{SI} decreases more rapidly with temperature than K_{MD}, the magnitude of the two anisotropy constants become equal at a given temperature (T_M), and the easy magnetic axis rotates by 90°. The crossover temperature has been shown to vary very sharply with a variety of factors, as impurities and doping,[25,27] particle size[28–32] or pressure.[33–35]

Fujii *et al.* have studied by Mössbauer spectroscopy the Morin transition of a 1000-Å-thick α-Fe_2O_3 film epitaxially grown on α-$Al_2O_3(0001)$.[36] They did not find any reorientational transition at least down to 2.5 K, the spin alignment remaining within the *c* plane. By x-ray diffraction, they detected that the 1000-Å-thick film exhibits a small expansion within the *c* plane and a small contraction within the *c* axis. Our 80-Å-thick film does not undergo the reorientational transition at least down to 125 K and it also presents a small expansion within the *c* plane. As a common feature of the 1000- and 80-Å-thick α-$Fe_2O_3(0001)$ layers is the expansion in the *c* plane with respect to the bulk, this expansion should be considered as an important factor responsible of the lowering of T_M. Finite size effects do not seem to be as important. Indeed, the film thicknesses (1000 and 80 Å) are significantly much larger than those of other AF films for which finite size effects have been evidenced.[12,13]

The lowering of T_M in thin layers can be discussed in the light of early papers concerning the magnetic properties of α-Fe_2O_3 microcrystals (1000–100 Å in diameter).[28–32] In small particles, it is systematically found that T_M decreases with the decrease in particle size. It is also well established that the rhombohedral lattice parameter increases ($\Delta a/a$ between 0.05% and 0.6%) when the particle diameter decreases.[29,30] Authors connect the lowering of T_M in microcrystals with the expansion of the cell parameter and consider that surface or finite size effects are of secondary importance. Indeed, it is well established elsewhere that there exist a strong interaction between the magnetic and the elastic subsystems in α-Fe_2O_3. Studies of the magnetoelastic interaction in hematite bulk samples have established that hydrostatic pressure raises T_M,[35] whereas mechanical stretching (''negative pressure effect''), which expands the lattice parameter, lowers it.[33]

For explaining the lowering of T_M in microcrystals in the AMF framework, it is assumed that the magnetoelastic interaction mainly affects the dipole-dipole interaction K_{MD}. K_{SI} is much less affected by lattice distortions, but highly sensitive to other factors as Fe substitution.[27] Indeed, K_{MD} is found very sensitive to the Fe^{3+} ion special position parameter.[26,34] Within this interpretational framework, the expansion of the atomic distances should change the Fe^{3+} ion special positions in the cell to such an extent that it makes K_{MD} the dominant anisotropy, even at very low temperatures. Therefore, the magnetic moments would remain pinned in the basal plane and no reorientational transition towards an easy *c* axis would occur.

This approach can be directly extended to explain the lowering of T_M in thin layers. The expansion of the rhombohedral *a* parameter (rhombohedral basis) in the microcrystals is of the same order of magnitude as the expansion in the *c* plane (hexagonal basis) measured in the thin films. Yamamoto showed that changes in K_{MD} induced by an expansion or a contraction within the *c* plane are about ten times larger than those induced by changes occurring along the *c* axis.[30] In this hypothesis, if we apply the relationship between $\Delta a/a$ and the decrease of ΔT_M in microcrystals given by Schoeer and Nininger,[29] we find that the measured value of $\Delta a_0/a_0 = 0.3\%$ is consistent with the observation of a lowering of T_M below 125 K.

The absence of any XMLD signal in the 20-Å-thick layer is actually more complex to explain, and may be understood as the combined effect of several factors.

First, this result is compatible with a reduction of the Néel temperature below 125 K ($T_N^{Bulk}=953$ K). It is reported in the literature that microcrystals of diameter smaller than ~100 Å exhibit superparamagnetic behavior.[28,30,37] In the case of very thin films, also finite size effects should actually play an important role in the lowering of T_N. From the simplest point of view, there are just not enough Fe^{3+} layers stacked along the *c* axis to develop the magnetic pattern defining the properties of bulk α-Fe_2O_3. Indeed, T_N is found to be a strong function of the layer thickness, and 20 Å correspond to the dimensions below which finite size effects have been found in other AF oxide films.[12,13] Alders *et al.* have studied the thickness dependence of the magnetic properties of NiO(100) layers by XMLD at the Ni L_2 edge.[12] The XMLD signal of the 10 ML (~20 Å) layer is much reduced in comparison with the 20 ML (~40 Å) film, while the 5 ML (~10 Å) film is in the paramagnetic state at room temperature.

In addition to finite size effects, magnetoelastic interactions should be an important ingredient in very thin films. A lowering of T_N has been recently measured in a $LaFeO_3$ strained film of 400 Å of thickness.[5] In the present study, the in-plane expansion (0.8%) is significant and then we can conceive that the associated magnetoelastic interaction strongly perturbs the long-range dipole-dipole interaction in such a way that even at 125 K the 20-Å-thick layer is in the paramagnetic state.

In addition, the lattice changes in the thin film can be anisotropic, i.e., the measured expansion in the *c* plane (0.8%) can be accompanied by a compression along the *c* axis.[36] This fact can cause a significant distortion of the FeO_6 octahedra, leading to changes in the local crystal field, which could reduce the magnetic moment of the high-spin state of the Fe^{3+} ion.[5] This possible reduction of the Fe^{3+} magnetic

moment could be a much important ingredient for explaining the absence of any XMLD signal in the 20-Å-thick layer.

IV. CONCLUSIONS

The present work confirms XMLD as a technique particularly well adapted for studying the magnetic properties of ultrathin AF oxide layers.

In the case of a 80-Å-thick layer, XMLD measurements strongly indicate the absence of the reorientational Morin transition at least down to 125 K ($T_M^{\mathrm{Bulk}} \sim 263\,\mathrm{K}$). This anomalous magnetic behavior is attributed to the lattice expansion in the *c* plane (0.3%). This expansion should change the Fe^{3+} ion special positions in the cell to such an extent that it makes the dipolar anisotropy the dominant term, even at very low temperature. The consequence is that the magnetic moments remain pinned in the basal plane and the easy magnetic axis cannot turn along the *c* axis.

In the case of a 20-Å-thick layer, we do not detect any XMLD signal even at very low temperature (125 K). This strong reduction of the Néel temperature ($T_N^{\mathrm{Bulk}} = 953\,\mathrm{K}$), is probably due to important magnetoelastic interactions, coming from the expansion of the lattice parameter in the *c* plane (0.8%). For this thickness, finite size effects should also play an important role. A decrease of the Fe^{3+} magnetic moment can also contribute to the absence of any magnetic signal in the 20-Å-thick layer. Indeed, anisotropic changes of the atomic distances can lead to a distortion of the FeO_6 octahedra, reducing the magnetic moment of the high-spin state Fe^{3+} via crystal-field effects.

In summary, the magnetic properties of thin epitaxial layers of hematite differ significantly from those established in bulk samples. It is of high interest to go further into their consequences for exchange biasing applications. The present results open the way to the possibility of tailoring the ordering temperatures and the easy magnetic axis in AF layers, playing with both strain and layer thickness.

ACKNOWLEDGMENTS

The authors are grateful to E. Guiot and M. Henriot for their help in the experiments. They acknowledge C. Laffon and P. Parent, and the staff of LURE for support.

*Corresponding author.

[1] B. Dieny, V. S. Speriosu, S. Metin, S. S. P. Parkin, B. A. Gurney, P. Baumgart, and D. R. Wilhoit, J. Appl. Phys. **69**, 4774 (1991).
[2] J. Nogués and I. K. Schuller, J. Magn. Magn. Mater. **192**, 203 (1999).
[3] N. C. Koon, Phys. Rev. Lett. **78**, 4865 (1997).
[4] M. D. Stiles and R. D. McMichael, Phys. Rev. B **60**, 12 950 (1999); R. A. Hyman, A. Zangwill, and M. D. Stiles, *ibid.* **60**, 14 830 (1999).
[5] J. Stöhr, A. Scholl, T. J. Regan, S. Anders, J. Lüning, M. R. Scheinfein, H. A. Padmore, and R. L. White, Phys. Rev. Lett. **83**, 1862 (1999).
[6] A. Scholl, J. Stöhr, J. Lüning, J. W. Seo, J. Fompeyrine, H. Seigwart, J. P. Locquet, F. Nolting, S. Anders, E. E. Fullerton, M. R. Scheinfein, and H. A. Padmore, Science **287**, 1014 (2000).
[7] F. Nolting, A. Scholl, J. Stöhr, J. W. Seo, J. Fompeyrine, H. Siegwart, J.-P. Locquet, S. Anders, J. Lüning, E. E. Fullerton, M. F. Toney, M. R. Scheinfein, and H. A. Padmore, Nature (London) **405**, 767 (2000).
[8] S. A. Chambers, Surf. Sci. Rep. **39**, 105 (2000).
[9] M. Sano, S. Araki, M. Ohta, K. Noguchi, H. Morita, and M. Matsuzaki, IEEE Trans. Magn. **34**, 372 (1998).
[10] J. A. Eaton and H. Morrish, J. Appl. Phys. **40**, 3180 (1969); Can. J. Phys. **49**, 2768 (1971); A. H. Morrish, *Canted Antiferromagnetism: Hematite* (World Scientific, Singapore, 1994).
[11] J. Baruchel, M. Schlenker, and S. B. Palmer, Nondestr. Test. Eval. **5**, 349 (1990).
[12] D. Alders, L. H. Tjeng, F. C. Voogt, T. Hibma, G. A. Sawatzky, C. T. Chen, J. Vogel, M. Sacchi, and S. Iacobucci, Phys. Rev. B **57**, 11 623 (1998).
[13] E. N. Abarra, K. Tanako, F. Hellman, and A. E. Berkowitz, Phys. Rev. Lett. **77**, 3451 (1996).
[14] C. G. Shull, W. Strausser, and E. O. Wollan, Phys. Rev. **83**, 333 (1951).
[15] R. Nathans, S. J. Pickart, H. A. Alperin, and P. J. Brown, Phys. Rev. **136**, 1641 (1964).
[16] J. C. Marmeggi, D. Hohlwein, and E. F. Bertaut, Phys. Status Solidi A **39**, 57 (1977).
[17] I. E. Dzialoshinskii, Zh. Eksp. Teor. Fiz. **33**, 1454 (1957) [Sov. Phys. JETP **6**, 1120 (1958)].
[18] T. Moriya, Phys. Rev. **120**, 91 (1960).
[19] F. J. Morin, Phys. Rev. **83**, 1005 (1951).
[20] P. Kuiper, B. G. Searle, P. Rudolf, L. H. Tjeng, and C. T. Chen, Phys. Rev. Lett. **70**, 1549 (1993).
[21] E. Guiot, S. Gota, M. Henriot, M. Gautier-Soyer, and S. Lefèbvre, in *Application of Synchrotron Radiation Techniques to Materials Science IV*, edited by S. M. Mini, D. L. Perry, S. R. Stock, and L. J. Termineilo, Mater. Res. Soc. Symp. Proc. No. 524 (Materials Research Society, Pittsburgh, 1998).
[22] E. Guiot, Ph.D. thesis, Université P. et M. Curie, 1998.
[23] S. Gota, E. Guiot, M. Henriot, and M. Gautier-Soyer, Phys. Rev. B **60**, 14 387 (1999).
[24] S. Gota, M. Gautier-Soyer, and M. Sacchi, Phys. Rev. B **62**, 4187 (2000).
[25] J. Baruchel, G. Clark, B. K. Tanner, and B. E. Watts, J. Magn. Magn. Mater. **68**, 374 (1987); V. V. Kvardakov, J. Sandonis, K. M. Podurets, S. Sh. Shilstein, and J. Baruchel, Physica B **168**, 242 (1991).
[26] J. O. Artman, J. C. Murphy, and S. Foner, Phys. Rev. A **138**, 912 (1965).
[27] P. J. Besser, A. H. Morrish, and C. W. Searle, Phys. Rev. **153**, 153 (1967); N. A. Curry, G. B. Johnson, P. Besser, and A. H. Morrish, Phys. Mag. **12**, 221 (1965).
[28] W. Kundig, H. Bommel, G. Constabaris, and R. H. Lindquist, Phys. Rev. **142**, 327 (1966).
[29] D. Schroeer and R. C. Nininger, Jr., Phys. Rev. Lett. **19**, 632 (1967); R. C. Nininger, Jr., and D. Schroeer, J. Phys. Chem. Solids **39**, 137 (1978).
[30] N. Yamamoto, J. Phys. Soc. Jpn. **24**, 23 (1968).

[31] G. J. Muench, S. Arajs, and E. Matijevic, Phys. Status Solidi A **92**, 187 (1985).
[32] N. Amin and S. Arajs, Phys. Rev. B **35**, 4810 (1987).
[33] N. Kawai, F. Ono, and K. Hirooka, J. Appl. Phys. **39**, 712 (1968).
[34] R. Z. Levitin, A. S. Pakhomov, and V. A. Shchurov, Zh. Eksp. Teor. Fiz. **56**, 1242 (1969) [Sov. Phys. JETP **29**, 669 (1969)].
[35] C. L. Bruzzone and R. Ingalls, Phys. Rev. B **28**, 2430 (1983).
[36] T. Fujii, M. Takano, R. Kakano, Y. Isozumi, and Y. Bando, J. Magn. Magn. Mater. **135**, 231 (1994).
[37] M. A. Polikarpov, I. V. Trushin, V. M. Cherepanov, and S. S. Yakimov, Fiz. Tverd. Tela (Leningrad) **33**, 2749 (1991) [Sov. Phys. Solid State **33**, 1554 (1991)].